Zoological Journal of the Linnean Society, 2023, XX, 1–12
https://doi.org/10.1093/zoolinnean/zlad183
Advance access publication 12 December 2023
Original Article

OXFORD

Original Article

The first record of the genus *Prosantorhinus* (Perissodactyla: Rhinocerotidae) of East Asia

Danhui Sun[1,2], Tao Deng[1,2,*], Shiqi Wang[2]

[1]University of Chinese Academy of Sciences Beijing 100049, China
[2]Key Laboratory of Vertebrate Evolution and Human Origins, Institute of Vertebrate Paleontology and Paleoanthropology, Chinese Academy of Sciences Beijing 100044, China

[*] Corresponding author. Key Laboratory of Vertebrate Evolution and Human Origins, Institute of Vertebrate Paleontology and Paleoanthropology, Chinese Academy of Sciences Beijing 100044, China, University of Chinese Academy of Sciences Beijing 100049, China. E-mail: dengtao@ivpp.ac.cn

ABSTRACT

Prosantorhinus is a genus of small extinct teleoceratine rhinoceroses with shortened limb bones, widely distributed in Europe. However, the Asian evolution of the teleoceratine *Prosantorhinus* has remained unclear because of a scarcity of fossil records of the genus. Here, we report the first record of *Prosantorhinus* in East Asia from the Middle Miocene of Tongxin, Ningxia. The new specimen is characterized by a concave dorsal skull profile and elevated nasals; short and stout nasal bones with drooping margins on both sides; the thickened, enlarged, and roughened nasal extremity supporting a small horn; the semi-molarized upper premolars with a lingual bridge between the protocone and hypocone; the metaloph constriction present on P2–4; the protocone equal to the hypocone on P2; the crista present on P3; and the cement on the cheek teeth developed. With all the morphological evidence considered, we establish a new species, *Prosantorhinus yei* sp. nov.. A phylogenetic analysis based on 282 morphological characters scored for 36 taxa reveals that *Prosantorhinus yei* sp. nov. is a relatively derived taxon in the genus. We hypothesize that *Prosantorhinus yei* sp. nov. lived in relatively moist environments.

Keywords: *Prosantorhinus*; Middle Miocene; phylogeny; palaeoecology; China

INTRODUCTION

Prosantorhinus Heissig, 1974 is a genus of small extinct teleoceratine rhinoceroses, having a concave dorsal skull profile with upslanting nasals and shortened limb bones (Cerdeño 1996, Heissig 2017). Heissig (1974) established the genus name *Prosantorhinus* for *Brachypodella germanica*, creating the new combination *Prosantorhinus germanicus* (Wang, 1929) based on the left maxilla fragment BSPG A.S.7 with P2–M3 from Georgensgmünd, southern Germany. *Prosantorhinus germanicus* is distributed in Germany and France along the Middle Miocene (MN 5–MN 7) (Heissig 1972, 2017, Cerdeño 1996). Osborn (1900) established the species *Diceratherium douvillei* based on the left maxilla fragment MNHN, Tav82 with P2–M2 discovered in Beaugency-Tavers, France, which was later classified as *Prosantorhinus douvillei* by Heissig (1972). *Prosantorhinus douvillei* was distributed in France, Spain, and Portugal from the Early to Middle Miocene (MN 3b–MN 7) (Cerdeño 1996). Heissig and Fejfar (2007) erected the species *Prosantorhinus laubei* according to some upper cheek teeth discovered in the Czech Republic. According to Heissig (2017), *P. laubei* was distributed in Ahníkov, the Czech Republic, and Wintershof-West, southern Germany, from the Early Miocene (MN 3a). Antoine *et al.* (2010) subsumed into *Prosantorhinus*, the small and short-legged species *P. shahbazi* (Pilgrim, 1910) from the Bugti area, Pakistan (~MN 2).

Prosantorhinus has undergone two revisions (Cerdeño 1996, Heissig 2017) since its establishment. The initial revision comprised only two well-defined species: *P. germanicus* (Wang, 1929) and *P. douvillei* (Osborn, 1900). Heissig (2017) published a more recent revision of the European species of *Prosantorhinus*, referring the species *Diceratherium aurelianense* to the genus *Prosantorhinus*, which was later overturned by Jame *et al.* (2019), who discussed the species in detail and considered *Diceratherium aurelianense* as a member of the genus *Diceratherium*. Heissig (2017) also referred to *Prosantorhinus*, with doubts, the species ?*P. tagicus* from the Early Miocene (MN 3a) of Lisbon (Portugal), which was previously identified as *Protaceratherium minutum* by Cerdeño (1996). Heissig (2017)

Received 13 May 2023; revised 8 November 2023; accepted 10 November 2023

emphasized that ?*P. tagicus* has a posterior hypocone furrow on the second molar, which is typical for many Teleoceratini, and a strong metacone fold on the ectoloph of the upper premolars, which are absent in Aceratheriini. Through the observation of ?*P. tagicus*, we did not see these distinctive features, therefore, we refer it to *Protaceratherium minutum* following Cerdeño (1996).

To date, the genus *Prosantorhinus* contains the following species: *P. germanicus* (Wang, 1929), *P. douvillei* (Osborn, 1900), *P. laubei* Heissig and Fejfar, 2007, and *P. shahbazi* (Pilgrim, 1910). The species of *Prosantorhinus* extend from the Early Miocene to the Middle Miocene (from the MN 2 to the MN 7/8 biozones), only distributed in Europe and Pakistan (Heissig 2017). Due to the scarcity of fossil records, the Asian evolution of *Prosantorhinus* remains unclear.

Here, we describe the first fossil record of *Prosantorhinus* in East Asia, represented by an adult teleoceratine skull (IVPP V 23530) from the Middle Miocene of Tongxin, Ningxia. The Tongxin area is in the southern part of Wuzhong City, Ningxia Hui Autonomous Region, China (Fig. 1A). The new fossil material of *Prosantorhinus* reported here was discovered in the middle layers of the Zhang'enbao Formation exposed in Lijiazhuang (Fig. 1B). Herein, we describe and compare this teleoceratine material in detail and discuss its phylogenetic relationship.

MATERIALS AND METHODS

The material basis for this study is an adult skull discovered in Tongxin, Ningxia Hui Autonomous Region, China, housed in the Institute of Vertebrate Paleontology and Paleoanthropology (IVPP), Chinese Academy of Sciences, Beijing, China. Rhinocerotid terminology and taxonomy follow Heissig (1972, 1999), Guérin (1980), and Antoine (2002). Anatomical features described follow the same sequence as in Antoine (2002) and Antoine *et al.* (2010). The specimen was measured in accordance with the procedures described in Guérin (1980).

The phylogenetic analysis is performed based on the data matrix from Antoine (2002, 2003) to assess the phylogenetic position of the new specimen. The matrix analysed in the present study contains 282 morphological characters, including 52 cranial characters, 10 mandibular characters, 120 dental characters, and 100 postcranial characters. The phylogenetic analysis was carried out via a heuristic search using PAUP4.0a169 (Swofford 2002), with tree-bisection-reconnection (reconnection limit = 8), 1000 replications with random addition sequence (10 trees held at each step), gaps treated as missing, and no differential weighting or topological constraint a priori. Except for characters 72, 94, 102, 140, and 187 (unordered), all multistate characters are treated as ordered. The current matrix consists of 36 taxa coded at the species-level with four outgroups [the extant tapirid *Tapirus terrestris* von Linnaeus, 1758, the Eocene hyrachyid rhinocerotoid *Hyrachyus eximius* Leidy, 1871 from North America, the Eocene rhinocerotid *Trigonias osborni* (Lucas, 1900) from North America, and the Oligocene rhinocerotid *Ronzotherium filholi* (Osborn, 1900) from Europe] and 32 ingroup taxa. We add *Brachydiceratherium shanwangense*, *Brachydiceratherium aginense*, *Brachydiceratherium aurelianense*, *Brachydiceratherium lemanense*, *Brachydiceratherium asphaltense*, *Alicornops simorrense*, *Diaceratherium tomerdingense*, *Brachypotherium perimense*, *Prosantorhinus germanicus*, *Prosantorhinus laubei*, and the new material into the matrix of Antoine (2002, 2003). In addition, Sizov *et al.* (2022) classified all species of *Diaceratherium* except the type species into *Brachydiceratherium*, indicating a complicated relationship of this genus, and put *D. tomerdingense* in the basal position of Teleoceratini.

Abbreviations

DP, Deciduous Premolar; M, Molar; P, Premolar.

MN, European Neogene Mammal Zones.

BSPG, Bayerische Staatssammlung für Paläontologie und Geologie, Münich, Germany; IVPP, Institute of Vertebrate Paleontology and Paleoanthropology, Chinese Academy of

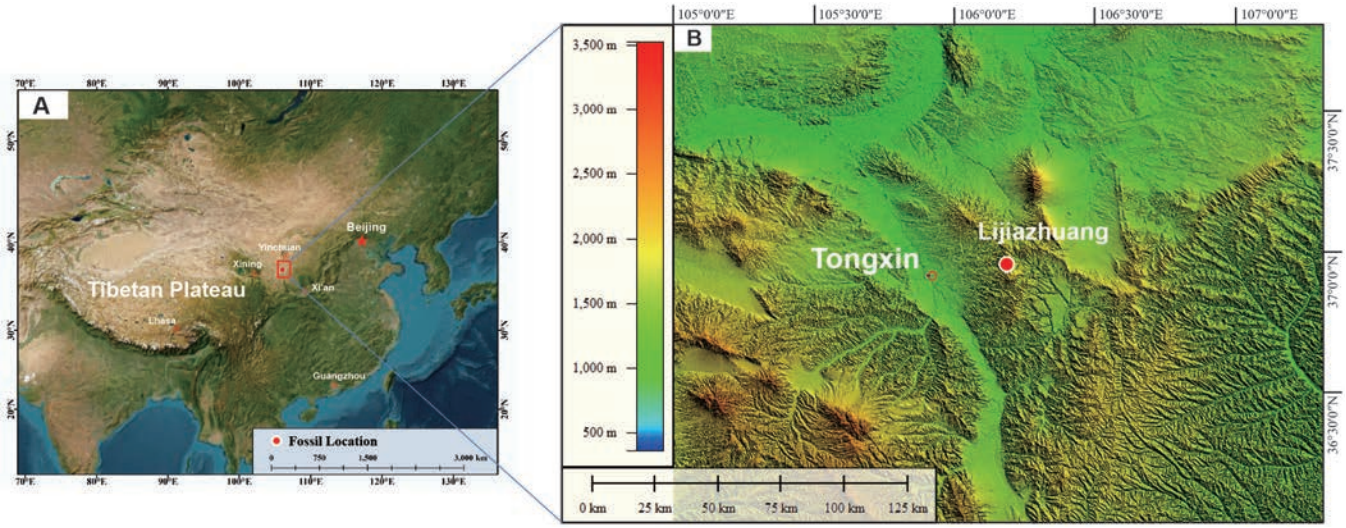

Figure 1. Geographic information of localities bearing *Prosantorhinus yei* sp. nov. in China. A, geomorphology of East Asia. B, fossil locality Lijiazhuang yielding *Prosantorhinus yei* sp. nov. from Tongxin.

Sciences, Beijing, China; MNHN, Muséum National d'Histoire Naturelle, Paris, France.

Systematic palaeontology

Order Perissodactyla Owen, 1848

Family Rhinocerotidae Gray, 1821

Tribe Teleoceratini Hay, 1902

Genus *Prosantorhinus* Heissig, 1974

Type species: *Prosantorhinus germanicus* (Wang, 1929).

Other species: *Prosantorhinus douvillei* (Osborn, 1900), *P. laubei* Heissig and Fejfar, 2007, *P. shahbazi* (Pilgrim, 1910), and *P. yei* sp. nov..

Revised diagnosis: Small- to medium-sized teleoceratines with concave dorsal skull profile and elevated nasals. The nasal extremity is thickened, enlarged, and roughened, which would support a small horn. The nasal incision is high and short. The zygomatic arches are high. Compared with the upper molars, the upper premolars are shortened. The crochet on the upper premolars usually presents two or more folds. M3 has a triangular outline and short distal cingulum. The cement on the buccal tooth walls is developed, but incomplete. The postcranials are robust. Manus tetradactyl to tridactyl. The second metatarsal with proximal articular facet shortened from the rear by a foramen nutritium (Cerdeño 1996, Heissig 2017).

Distribution: Early to Middle Miocene (MN 2–7/8), western and central Europe, as well as southern and eastern Asia.

Prosantorhinus yei sp. nov.

(Figs 2–6; Tables 1–3)

Zoobank registration: urn:lsid:zoobank.org:pub:A307A235-FB07-41FF-AD68-3DA0FF60BA94.

Holotype: IVPP V 23530, a well-preserved and complete skull with both cheek tooth rows (left and right DP1–M3) (Figs 2–4).

Diagnosis: The V-shaped nasal notch with its posterior edge at the level of the middle part of P3 and anterior margin of the orbit located at the level of the anterior edge of M1 differs from *P. douvillei*. The upper premolars are semi-molarized with a lingual bridge between the protocone and hypocone different from *P. germanicus*, *P. laubei*, and *P. douvillei*. The strong constrictions of the protocone, as well as stout antecrochet and crochet on molars, differ from *P. laubei* and *P. shahbazi*. The multiple crochet on the upper premolars and the present crista on P3 differ from *P. germanicus*, *P. laubei*, and *P. douvillei*. The cement on the cheek teeth is developed differently from *P. germanicus*, *P. laubei*, and *P. douvillei*.

Etymology: The species' name is in honour of Professor Jie Ye, who has made great contributions to Neogene palaeontology and stratigraphy in the Tongxin area.

Type locality and horizon: Zhang'enbao Formation exposed in Lijiazhuang in Shishi Township, Tongxin County, Wuzhong City, Ningxia Hui Autonomous Region, China; Middle Miocene.

Description

Cranium: IVPP V 23530 is a well-preserved and complete adult skull with moderately worn cheek teeth (Fig. 2). In the dorsal view (Fig. 2A), the nasal suture between both nasals is observable, and the rostral end of the nasal bone is very rugose, indicating the presence of a nasal horn. The nasal bone becomes narrow gradually before the orbits (i.e. the nasal base does not have a constriction). The skull roof has the widest distance at the level of the supraorbital processes, at 154.96 mm. The parietal crests are not fused to a sagittal crest, and the minimal separation is 46.28 mm. The width of the occipital crest is 137.32 mm. In the lateral view (Fig. 2B), the dorsal skull profile is concave. The nasal bone has a slightly upturning anterior part, and the occipital part is raised. The premaxillae are not preserved. The nasal bone is short and stout. The nasal notch has a V-shaped outline, and its posterior edge is at the level of the middle part of P3. The distance between the posterior edge of the nasal notch and the orbit is 71.32 mm. The infraorbital foramen is located dorsal to the level of P3 and behind the nasal notch. The position of the dorsal margin of the orbit is high, and the anterior margin of the orbit is located at the level of the anterior edge of M1. The supraorbital edge of the frontal bone has a coarse area, but lacks any process or tubercle. The posterior orbital border is formed by the zygomatic bone, and presents a coarse area, without any tubercle. The zygomatic arch is thin (particularly the posterior part), the anterior end of which is located at the level of M1 and close to the cheek tooth row, and the posterior end of the dorsal edge has a short process. The temporal articulation for the mandible protrudes from the ventral edge of the zygomatic arch. The postglenoid process is laterally flattened. The occipital part is raised, with the occipital face slightly inclined anteriorly in lateral view. The post-tympanic process is short and fused with the paraoccipital process, and contacts anteriorly with the postglenoid process. The upper edge of the external auditory pseudomeatus is short and located in the lower half of the occipital crest. The area between the temporal and occipital crests is depressed. In the ventral view (Fig. 2C), the medial edge of the cheek tooth row is nearly straight, and the lateral edge is arched. The anterior edge of the posterior nares is U-shaped in outline, at the level between M2 and M3. The posterior edge of the lateral wall of the posterior nares with a steep part is continuous, extending to the foramen lacerum anterius that is at the back of the level of the temporal condyle. The temporal condyle is high, and its transverse axis is concave posteriorly. The tympanic bulla has been crushed, exposing the inner bones. The alar foramen is opened on the lateral wall of the posterior nares, anteroposteriorly at the level of the temporal condyle. The post-tympanic process is wide, transversely extending to the level of the lateral half of the temporal condyle. The hypoglossal foramen is laterally positioned, at the base of the paraoccipital process. The ventral and occipital surfaces of the occipital condyle are rounded, without a median ridge. In the posterior view (Fig. 3), the occipital face is trapezoidal in outline, and the upper part is slightly narrower than the lower part. The nuchal tuberosity is strongly developed. There is a shallow notch between the base of the paraoccipital process and the post-tympanic process. The foramen magnum is small, triangular, and higher than wide. The upper margin of this foramen is narrow, inverted V-shaped, and higher than the upper margin of the occipital condyles. The occipital condyles are relatively small (Table 1).

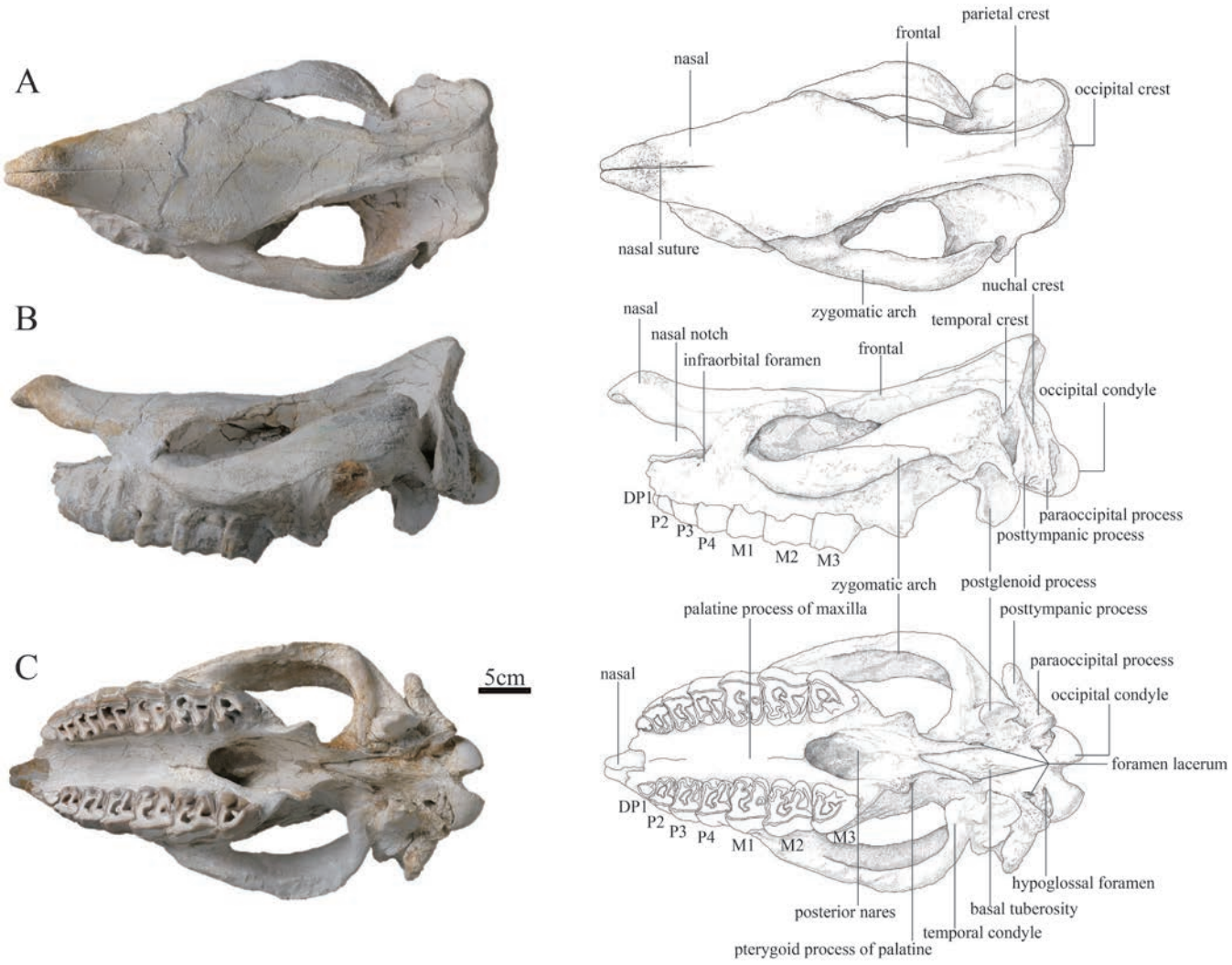

Figure 2. Photographs and sketches of the skull of *Prosantorhinus* yei sp. nov., holotype (IVPP V 23530) A, dorsal view; B, lateral view; C, ventral view.

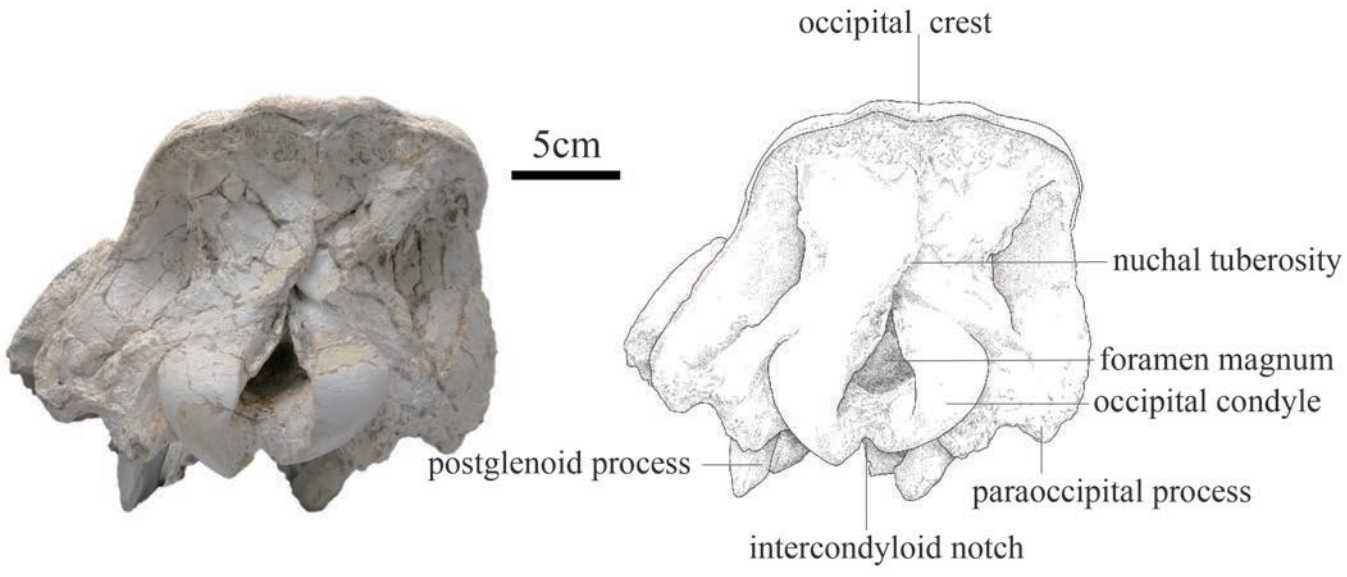

Figure 3. Photograph and sketch of the skull of *Prosantorhinus yei* sp. nov., holotype (IVPP V 23530).

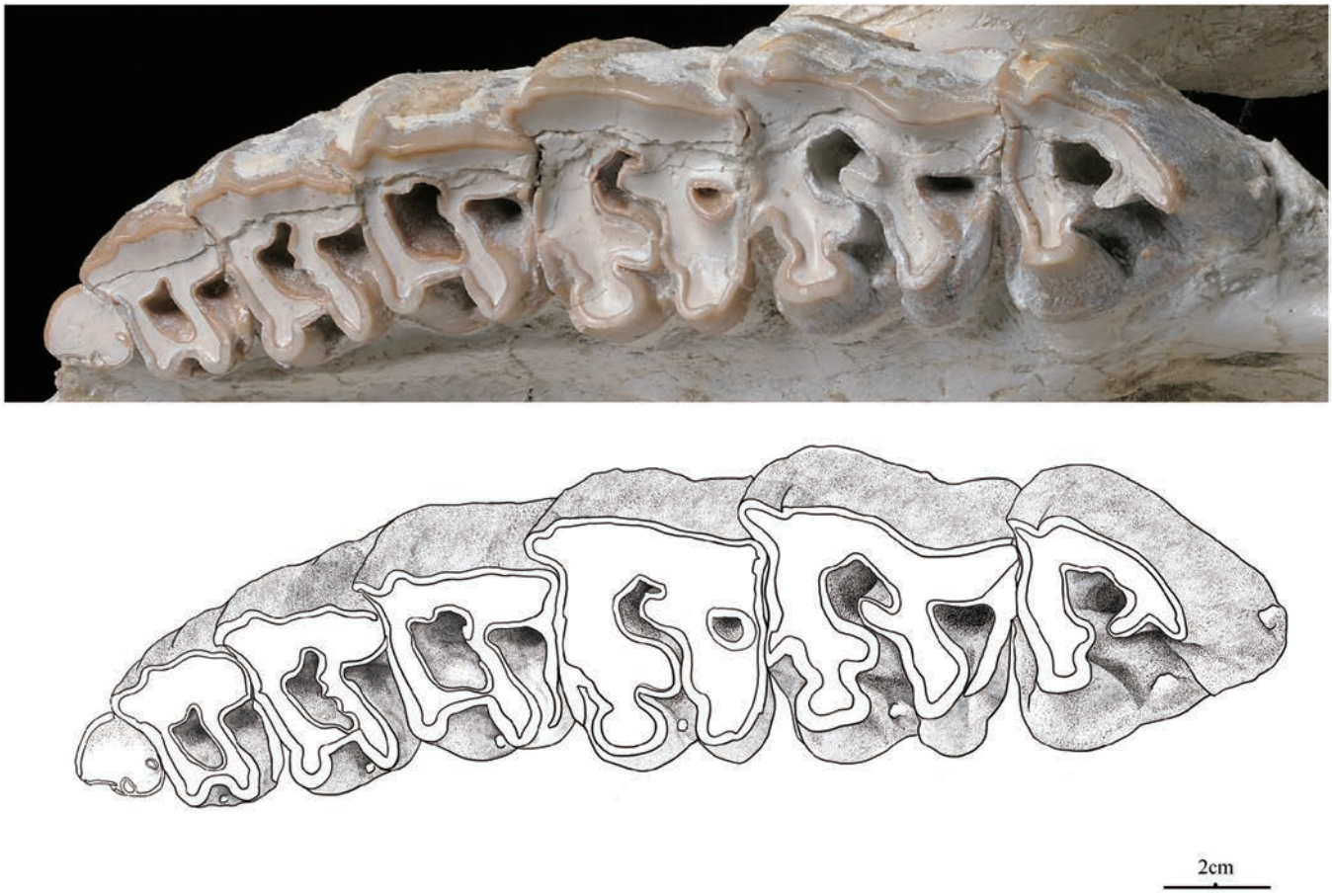

Figure 4. Photograph and sketch of upper teeth (IVPP V 23530) of *Prosantorhinus yei* sp. nov. in occlusal view, holotype (IVPP V 23530).

Dentition: The cheek teeth have relatively low crowns, covered by abundant cement on the buccal walls and they are moderately worn (Fig. 4; Table 2). The ratio of the length of the upper premolars (P3–4) to the molars (M1–3) is high, more than 50%.

DP1 is fairly small and deeply worn to a flat surface with a triangular outline; the protoloph is weak and nearly worn off; the metaloph is developed; the hypocone has slight anterior and posterior constrictions; the postfossette is closed; the lingual cingulum is present, but the buccal cingulum is absent.

P2 is nearly quadrangular in occlusal view with a parastyle and comparatively developed paracone rib. The protocone and hypocone, with slight constrictions, connect by a lingual bridge. The hypocone is marginally larger than the protocone. The hypocone is at the same level as the metacone. The protoloph is as buccally narrow as the metaloph and joins with the ectoloph. The crochet and crista are very weak. Both the median valley and the postfossette are closed. The anterior and the posterior cingula are developed. The lingual cingulum is reduced around the entrance of the median valley. The buccal cingulum is absent. The cement on the buccal surface is abundant.

P3 has marked paracone and metacone ribs. The protocone has anterior and posterior constrictions, and the hypocone only has a slight anterior constriction. The protocone and hypocone connect by a lingual bridge. The protocone is slightly larger than the hypocone. The crochet and crista are weak, and the crochet is multiple. The median valley and postfossette are closed. The lingual margin of the protocone is convex. The anterior and posterior cingula are developed, but the lingual cingulum is reduced around the entrance of the median valley. The buccal cingulum is reduced.

P4 is similar to P3, but much larger. The hypocone is not expanded, with slight anterior and posterior constrictions. The protocone is slightly smaller than the hypocone. The lingual margin of the protocone is convex. The protoloph is shorter than the metaloph. The anterior and posterior cingula are developed, but the lingual cingulum is reduced, forming a pillar around the entrance of the median valley. The buccal cingulum is almost absent.

M1, with an undulating buccal wall, has a projecting parastyle, a marked parastyle groove, and a paracone rib. The strongly constricted protocone has a convex lingual margin, and the hypocone only has a slight anterior constriction. The crochet is short and stout. The antecrochet is strong and extends to the entrance of the median valley. The postfossette is round. The development of anterior and posterior, as well as lingual and buccal, cingula are similar to P4.

M2 has a narrow and long parastyle, a developed parastyle groove, and a paracone rib. The protocone is expanded, with anterior and posterior constrictions. The hypocone only has a slight anterior constriction. The crochet is well-developed. The antcrochet is strongly developed and extends to the entrance of the median valley. The antecrochet and hypocone are

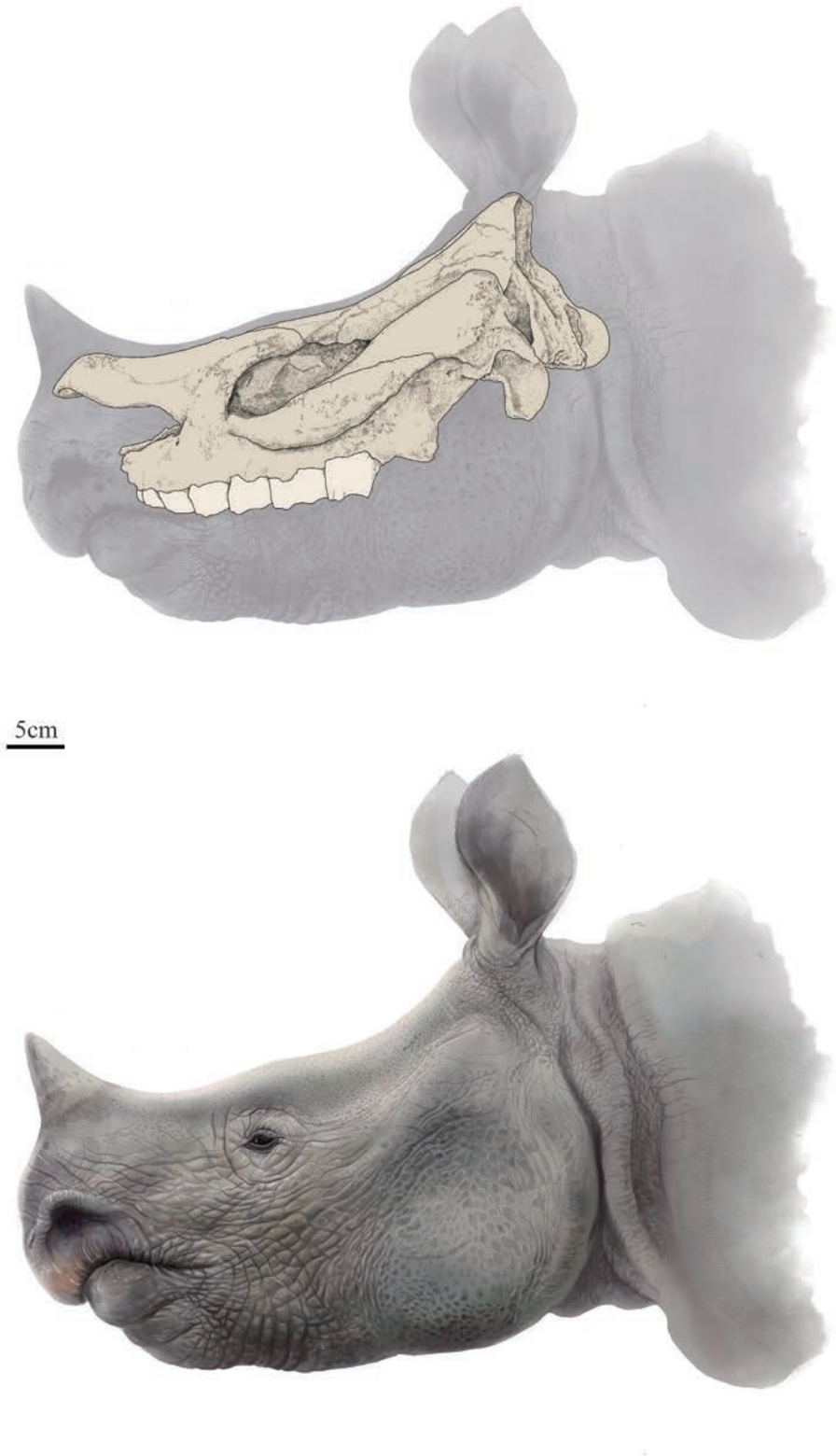

Figure 5. The reconstruction of *Prosantorhinus yei* sp. nov..

separated. M2 has an open median valley, a V-shaped and closed postfossette, and a relatively narrow and long metastyle. The development of anterior and posterior, as well as lingual and buccal, cingula are similar to P4 and M1.

M3 has a triangular outline in occlusal view. It has a short and sharp parastyle. The protocone has anterior and posterior constrictions. The protoloph is anteriorly convex. The crochet is well-developed but does not reach the protoloph. There is a reduced antecrochet that enlarges to the base of the crown. The anterior cingulum is well developed, and the posterior and lingual cingula are reduced, forming a pillar.

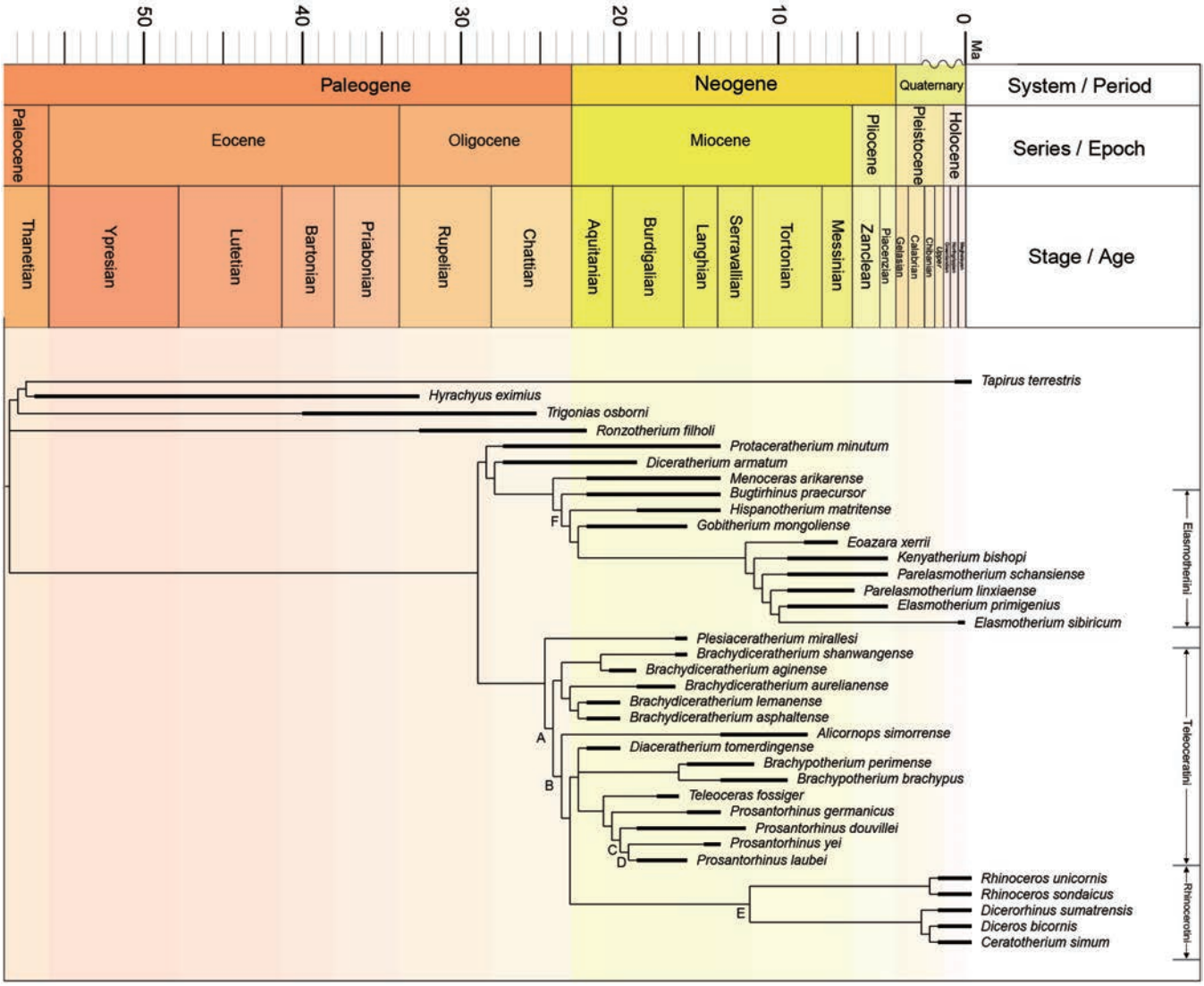

Figure 6. Strict consensus of two most parsimonious trees, with 1450 steps in PAUP (consistency index = 0.2669; retention index = 0.5157), showing systematic position of *Prosantorhinus yei* sp. nov. For convenience, capital letters (A–F) below the branches are used to denote monophyletic groups discussed in the text.

DISCUSSION

Morphological comparison

The skull (IVPP V 23530) from Tongxin, Ningxia can be easily differentiated from other Eurasian rhinocerotids as follows. The lack of developed enamel folds and developed cement in the middle valley on upper teeth differ from elasmotheres, which include gracile rhinoceroses with cemented and hypsodont cheek teeth (Deng 2003, Sun *et al.* 2023); the single small horn boss on the nasal bone is distinctly different from both menoceratines, with a pair of nasal horns, and rhinocerotines with a relatively larger nasal horn (Prothero 2005). The obvious horn boss on a short and stout nasal bone is different from *Shansirhinus*, an aceratheriine that develops nasal horn, with slightly upturned nasal bone (Deng 2005). In contrast, the Tongxin specimen is easily recognizable as a typical teleoceratine, notably *Prosantorhinus*, due to the medium size, concave dorsal skull profile and elevated nasals, nasal notch moderately retracted at the P3 level, high zygomatic arches, raised occipital bone, semi-molarized upper premolars, and a strong antecrochet on the upper molars (Heissig 1972, 2017, Cerdeño 1996, Heissig and Fejfar 2007).

The tribe Teleoceratini was established based on the genus *Teleoceras* from the Late Miocene of North America (Prothero 2005). The Tongxin specimen is small-sized with low crown cheek teeth, while *Teleoceras* is medium- to large-sized with hypsodont teeth, with less abundant cement on teeth, and wider zygomatic arches. Compared with other Teleoceratini, the Tongxin specimen differs from *Aprotodon* (Qiu *et al.* 2004) in having a nasal horn boss. The largest European *Brachypotherium* has a straight skull profile and short narrow nasals with occasionally a feeble horn (Geraads and Miller 2013), different from the Tongxin specimen (Table 3). The genus *Diaceratherium*, widely distributed throughout Eurasia, has recently been restricted to the species *Diaceratherium tomerdingense* and the other species of this genus have now been referred to *Brachydiceratherium* (Sizov *et al.* 2022). The Tongxin specimen is smaller than *Brachydiceratherium*, which is medium- to large-sized (Jame *et al.* 2019) (Table 3).

Table 1. Measurements of the skull (IVPP V 23530) of *Prosantorhinus yei* sp. nov. from Tongxin, Ningxia, measurements in milimetres.

Numbers	Measures	IVPP V 23530
1	Distance between occipital condyle and premaxilla	-
2	Distance between occipital condyle and nasal tip	517.02
3	Distance between nasal tip and occipital crest	472.82
4	Distance between nasal tip and bottom of nasal notch	123.21
5	Minimal width of braincase	47.83
6	Distance between occipital crest and postorbital process	233.82
7	Distance between occipital crest and supraorbital process	257.96
8	Distance between occipital crest and lacrimal tubercle	288.76
9	Distance between nasal notch and orbit	71.32
13	Distance between occipital condyle and M3	240.23
14	Distance between nasal tip and orbit	203.18
15	Width of occipital crest	137.32
16	Width of paramastoid process	213.86
17	Minimal width between parietal crests	46.28
18	Width between postorbital processes	147.52
19	Width between supraorbital processes	154.96
20	Width between lacrimal tubercles	134.39
21	Maximal width between zygomatic arches	63.72
22	Width of nasal base	102.42
23	Height of occipital surface	106.44
25	Cranial height in front of P2	105.34
26	Cranial height in front of M1	109.42
27	Cranial height in front of M3	121.26
28	Width of palate in front of P2	45.42
29	Width of palate in front of M1	54.21
30	Width of palate in front of M3	59.78
31	Width of foramen magnum	34.41
32	Width between exterior edges of occipital condyle	99.53

In contrast, there are clear similarities with the type species of *Prosantorhinus*, *P. germanicus*, in the molars, but there are many differences in the premolars. For instance, the premolars of the Tongxin specimen are semi-molarized with a lingual bridge between the protocone and hypocone, while those of *P. germanicus* are molarized. The Tongxin specimen has a relatively weaker paracone rib than that of *P. germanicus*, and the cheek teeth are covered by abundant cement on the buccal wall, while cement is almost absent in *P. germanicus*.

It also differs from *P. douvillei*, in which the nasal notch is quite short, ending above P2. The anterior margin of the orbit of the Tongxin specimen is located at the level of the anterior edge of M1, whereas that of *P. douvillei* is located above the P3–4. The zygomatic arches of the Tongxin specimen are slenderer than those of *P. douvillei*. Premolars of the Tongxin specimen are semi-molarized with lingual bridge between the protocone and hypocone, but those of *P. douvillei* are molarized with separate protocone and hypocone. The hypocone on premolars of the Tongxin specimen has slightly constrictions different from that of *P. douvillei* without constriction. The crochet on the molar of the Tongxin specimen is well-developed and stronger than that of *P. douvillei*. Both species have short and multiple crochets on the premolars, but the crochet on the molars of *P. douvillei* is stronger.

Compared with *P. laubei*, the premolars of the Tongxin specimen are semi-molarized with a lingual bridge between the protocone and hypocone, while those of *P. laubei* are partly semi-molarized. The constrictions of the protocone on the molars are stronger than those of *P. laubei*. The hypocone on the molars has a slight anterior constriction that is not developed on those of *P. laubei*. The antecrochet and crochet on the molars are clearly more developed and stouter than in *P. laubei*. The cheek teeth of *P. laubei* lack cement.

The referred material of *P. shahbazi* (Pilgrim, 1910) from the Early Miocene of Pakistan is quite restricted (Antoine *et al.* 2010, 2013), but differences with IVPP V 23530 are obvious. The crochet on the molars of the Tongxin specimen is better developed and stronger than that of *P. shahbazi*. The lingual cingulum is more developed in *P. shahbazi*. The constrictions of protocone and hypocone and the antecrochet are stronger in the Tongxin specimen than those of *P. shahbazi*.

With all the morphological evidence considered, the new material from Tongxin (IVPP V 23530) differs from all the known species of this genus (Table 3) and is herein proposed as a new species, *Prosantorhinus yei* sp. nov. (Fig. 5).

Phylogenetic analysis

The performed phylogenetic analysis of the Rhinocerotidae [based on the data matrix of Antoine (2002, 2003), with

Table 2. Measurements of the upper teeth (IVPP V 23530) of *Prosantorhinus yei* sp. nov. from Tongxin, Ningxia compared with other *Prosantorhinus*, measurements in milimetres.

Teeth		*P. yei* sp. nov. IVPP V 23530	*P. germanicus* (Heissig 2017)	*P. laubei* (Heissig 2017)	*P. douville* (Heissig 2017)
DP1	L	16.91	-	-	-
	W	16.32	-	-	-
	H	7.29	-	-	-
P2	L	26.82	20.50	-	25.50
	W	31.82	23.00	-	32.50
	H	14.43	-	-	-
P3	L	33.07	26.50	30.00	28.00
	W	38.41	35.50	38.00	37.50
	H	23.42	-	-	-
P4	L	35.91	29.00	32.00	32.00
	W	42.54	40.50	>40	41.00
	H	30.17	-	-	-
M1	L	42.02	33.00	37.00	39.00
	W	50.57	40.50	43.00	40.00
	H	22.18	-	-	-
M2	L	49.35	38.00	-	40.50
	W	51.53	42.00	-	43.50
	H	34.29	-	-	-
M3	L	33.66	36.50	39.50	41.00
	W	47.84	38.50	45.50	40.50
	H	38.12	-	-	37.50

Table 3. Cranial characters of different species of *Prosantorhinus*, compared with *Diceratherium* and *Brachypotherium*.

Genus/species	*Diceratherium*	*P. yei* sp. nov.	*P. douvillei*	*P. germanicus*	*P. laubei*	*Brachypotherium*
Distal limb segments	long		short	very short	-	short
Fronto-nasal profile	straight	concave	concave	concave	-	straight
Nasal incision	P4–M1	P3	P3	P3	-	P4–M1
Nasals	long	medium	medium	medium	-	short
Horn base	small	medium	stronger	very strong	-	reduced or lacking
Anterior orbit rim above	M2	M1	M1	P4/M1	-	M1–M2
Premolars	semi-molarized	totally semi-molarized	partly semi-molarized	molarized	molarized	molarized
Cheek teeth	without cement	abundant cement	without cement	without cement	without cement	without cement

the addition of *Prosantorhinus yei* sp. nov., *P. germanicus*, *P. laubei*, the type species of *Diceratherium*, and some species of *Brachydiceratherium*] resulted in two equally most-parsimonious trees. The tree length is 1450 steps, with a consistency index of 0.2669 and a retention index of 0.5157.

Rhinocerotinae (Node A) include Teleoceratini and Rhinocerotini (Fig. 6). They share 33 unequivocal synapomorphies (Supporting Information, Appendix S1). The members of Teleoceratini are arranged as follows: [*Brachydiceratherium shanwangense*, *Brachydiceratherium aginense*, *Brachydiceratherium aurelianense*, *Brachydiceratherium lemanense*, *Brachydiceratherium asphaltense* [*Alicornops simorrense* [*Diceratherium tomerdingense* [*Brachypotherium perimense*, *Brachypotherium brachypus* [*Teleoceras fossiger* [*Prosantorhinus germanicus* [*Prosantorhinus douvillei* [*Prosantorhinus yei*, *Prosantorhinus laubei*]]]]]]]. The phylogenetic position of *Brachydiceratherium shanwangense*, *B. aginense*, *B. aurelianense*, *B. lemanense*, and *B. asphaltense* are consistent with the phylogenetic results of Sizov *et al.* (2022). *Alicornops*, a genus with a medium-sized skull and moderately specialized cheek teeth (Cerdeño and Sanchez 2000,

Deng 2004), had been referred to Aceratheriini for a long time (Prothero *et al.* 1986, Cerdeño 1995), but Lu *et al.* (2023) recently considered *Alicornops* as a sister-group of Teleoceratini. Its phylogenetic position (Node B) here is consistent with the phylogenetic result of Lu *et al.* (2023). The Node B is supported by 18 unequivocal synapomorphies (Supporting Information, Appendix S1).

The members of *Prosantorhinus* form a monophyletic lineage (Node C) supported by eight unequivocal synapomorphies, including absent i1, always absent constriction of the protocone on P3–4, continuous metaloph on M2, always absent constriction of the protocone on M3, usually present labial cingulum on lower molars, always present lingual groove on the entoconid on d3, usually present trapezium-facet of McII, always high and narrow expansion of the calcaneus-facet 1 of astragalus. *Prosantorhinus yei* nov. sp. established here forms a clade (Node D) with *Prosantorhinus laubei* (Fig. 6). Node D is supported by 12 unequivocal synapomorphies, including the depressed area between temporal and nuchal crests, foramen postglenoideum close to the processus postglenoidalis, the absent median ridge on the condyle, present cement on cheek teeth, wrinkled shape of enamel on cheek teeth, protoloph joined to the ectoloph on P2, always present antecrochet on upper molars, always present lingual cingulum on upper molars, narrow lingual opening of the postfossette on lower premolars, absent labial cingulum on lower premolars, always open postfossette on d2, and always high and narrow expansion of the calcaneus-facet 1 on astragalus. *Prosantorhinus yei* is supported by eight unequivocal autapomorphies: high crown of cheek teeth, present metaloph constriction on P2–4, the protocone equal to the hypocone on P2, usually present constriction of the protocone on P3–4, the lingual bridge between protocone and hypocone on P3–4, always present crista on P3, absent metacone fold on M1–2, always present constriction of the protocone on M3. *Prosantorhinus douvillei* is supported by 12 unequivocal autapomorphies, including always absent labial cingulum on upper premolars, usually present crochet on P2–4, continuous lingual cingulum on P2–4, usually absent lingual cingulum on upper molars, constricted metaconid on lower cheek teeth, always closed posterior valley on p2, always present lingual cingulum on lower molars, always present labial cingulum on lower molars, present lingual groove of the entoconid on m2–3, always closed posterior valley on d2, usually fused proximal ulna-facets of radius, vestigial McV. *Prosantorhinus laubei* is supported by three unequivocal autapomorphies: usually simple crochet on P2–4, usually absent antecrochet on P2–3, quadrangular shape of M3. The clade (Node E) containing Rhinocerotina is supported by 31 unequivocal synapomorphies (Supporting Information, Appendix S1). The clade (Node F) containing elasmotheres is supported by 41 unequivocal synapomorphies (Supporting Information, Appendix S1).

Based on the morphological comparison and the phylogenetic analysis, *Prosantorhinus yei* sp. nov. is more derived than the other species by the following features. The cheek teeth cement, metaloph constriction on P2–4, constriction of the protocone on P3–4, and crista on P3 of *P. yei* sp. nov. are characters absent in *P. germanicus*, *P. douvillei*, and *P. laubei*. The labial cingulum on the upper molars and metacone fold on M1–2 are absent in *P. yei* sp. nov., but present in *P. germanicus*. The antecrochet on the upper molars is present in *P. yei* sp. nov., *P. douvillei*, and *P. laubei*, but absent in *P. germanicus* . The constriction of the protocone on M3 is absent in *P. germanicus*, *P. douvillei*, and *P. laubei*. However, *P. yei* sp. nov. keeps some primitive features, such as semi-molarized premolars with a lingual bridge between protocone and hypocone, while premolars of *P. germanicus* and *P. laubei* are molarized with protocone and hypocone separated, and those of *P. douvillei* are partly semi-molarized.

Palaeoecology

As a teleoceratine rhinoceros, a hippo-like mode of life was assumed for *Prosantorhinus germanicus* (Heissig, 1999). In addition, Schellhorn and Schlösser (2021) compared the bone compactness data for the metacarpals in their study resulting that the bone compactness values of *P. germanicus* are close to the pygmy hippo data. According to Heissig (1972), three Sandelzhausen rhinoceros taxa are faunal elements of moist environments, but *P. germanicus* inhabited moister environments than *Plesiaceratherium fahlbuschi* and *Lartetotherium sansaniense*. Moreover, most species in the genus *Prosantorhinus* have low-crowned cheek teeth, which typically imply a diet of not abrasive plants with relatively high nutritional content, indicating that these animals are mostly browsers (Heissig 1999, 2017). This is generally confirmed by the form of the wear surface of the upper molars (Fortelius and Solounias 2000). Furthermore, Tütken and Vennemann (2009) analysed the carbon, oxygen, and strontium isotope composition of enamel from the teeth of large Miocene herbivorous mammals, and their results showed that *P. germanicus* was a browser in more closed forest environments. Schellhorn (2021) discussed in detail the carpal bone condition in *Prosantorhinus* with an additional palmar articulation resulting in a stiffening of the mid-carpal joint. The stiffening can also be interpreted in favour of a semi-aquatic mode of life. The stiffened carpus is more resistant against injuries while walking on muddy grounds in a wet environment.

From the perspective of a sedimentary environment, the Tongxin area was mainly influenced by a fluvial sedimentary environment, and there should be river(s) flowing through the area (Wang *et al.* 2016). In addition, the palynological comprehensive analysis shows that the Tongxin area is a flood-plain depositional environment, and *Artemisia*-dominated grassland with a small amount of coniferous and broad-leaved forest components (Wang 2021). A primate that accompanies *P. yei* sp. nov., *Pliopithecus zhangxiangi* (Harrison *et al.* 1991), has been reported, which also suggests a forested environment.

Based on the above evidence, we summarize that *Prosantorhinus*, with its short limbs and the proportions of its skull, may be correlated with habitat predilection for ponds and rivers, along with a strong need for moisture and water (Heissig 1999). Among mammals, and rhinos in particular, cranial characters (Schellhorn 2018) show adaptations to the environment. Schellhorn (2018) mentioned that a backward-inclined occiput implies a downward hanging head (often found in grazers), a forward-inclined occiput is related to the horizontal head posture in browsing rhinos. *Prosantorhinus yei* sp. nov. has an anteriorly inclined occiput with relatively low crown and semi-molarized premolars, suggesting that it is a browser. As a result, we hypothesize that *Prosantorhinus yei* sp. nov. lived in relatively moist environments.

Bugti documents the earliest occurrences of *Prosantorhinus*, with *P. shahbazi* from MN 2 (Antoine *et al.* 2010, 2013). The members of the genus *Prosantorhinus* range in size from very small to large species, including *P. laubei* from MN 3 of northern Bohemia and possibly in southern Germany (Heissig and Fejfar 2007, Heissig 2017), *P. douvillei* from MN 3–7/8 of France, Spain, and Portugal (Heissig 1972, 2017, Cerdeño 1996), and *P. germanicus* from MN 5–7 of Germany and France (Heissig 1972, 2017). Combined with the geological age of the layer where the fossil is located, we speculate that *P. yei* sp. nov. lived in the Middle Miocene (Wang *et al.* 2016).

Therefore, *Prosantorhinus* has a huge geographical range, extending from Western and Central Europe to southern Pakistan and China. The ubiquitous distributions of most teleoceratine taxa probably underline ultra-generalist ecological preferences (Hullot *et al.* 2021). Moreover, such ranges seemingly support the absence of efficient ecological and geographical barriers at the Eurasian scale for the concerned teleoceratines, at least by early Middle Miocene times. We speculate that the expansion of the genus *Prosantorhinus* was related to abiotic events. For instance, global climate changes occurred during the Miocene. In particular, the Middle Miocene Climate Optimum was the warmest period of the Cenozoic since the Late Eocene (Zachos *et al.* 2001, 2008, You *et al.* 2009). Suitable environments facilitate the dispersal and migration of animals.

CONCLUSION

The studied material from Tongxin, Ningxia is a well-preserved skull of rhinoceros (IVPP V 23530) identified as a teleoceratine of the genus *Prosantorhinus*. It differs from *Prosantorhinus germanicus* in having semi-molarized premolars and abundant cement on the buccal wall; from *P. douvillei* in a V-shaped nasal notch with its posterior edge at the level of the middle part of P3, the anterior margin of the orbit at the anterior level of M1, more slender zygomatic arches, and semi-molarized premolars; from *P. laubei* in having semi-molarized premolars, stronger constrictions of the protocone on molars, developed and stout antecrochet and crochet on the molars, and abundant buccal cement; from *P. shahbazi* in having well-developed and stronger crochet on molars, reduced lingual cingulum, stronger constrictions of protocone and hypocone, and strongly developed antecrochet on the molars.

Based on the aforementioned combination of characteristics, we herein establish the new species *Prosantorhinus yei* sp. nov.. The phylogenetic analysis supports the position of IVPP V 23530 as a species of *Prosantorhinus*, in a derived position, as sister-taxon of *P. laubei*. The new species complements the morphological characteristics of the *Prosantorhinus*, and enlarges the geographical distribution of the genus during the Middle Miocene, being the easternmost Eurasian record of the genus.

SUPPLEMENTARY DATA

Supplementary data are available at *Zoological Journal of the Linnean Society* online.

ACKNOWLEDGEMENTS

We thank Xiaocong Guo for her illustrations, Wei Gao for his photographs, Dan Su for her assistance in the repair of the fossil, and Thomas Stidham for assistance with manuscript editing. We are very grateful to the Editor Jeff Streicher, Associate Editor and four anonymous reviewers for their constructive comments and criticisms. This research was supported by the National Natural Science Foundation of China (42302013), the Second Comprehensive Scientific Expedition on the Tibetan Plateau (2019QZKK0705), and the National Key Research and Development Program of China (No. 2023YFF0804500).

CONFLICT OF INTEREST

None declared.

DATA AVAILABILITY

The specimen (IVPP V 23530) is housed in the Institute of Vertebrate Paleontology and Paleoanthropology, Chinese Academy of Sciences, Beijing, China. Supporting data (data matrix) for phylogenetic analyses in this study are provided in Supplementary Information.

REFERENCES

Antoine PO. *Phylogénie et Évolution des Elasmotheriina (Mammalia, Rhinocerotidae)*. Mémoires du Muséum National d'Histoire Naturelle 2002;1–359.

Antoine PO. Middle Miocene elasmotheriine Rhinocerotidae from China and Mongolia: taxonomic revision and phylogenetic relationships. *Zoologica Scripta* 2003;**32**:95–118. https://doi.org/10.1046/j.1463-6409.2003.00106.x

Antoine PO, Downing KF, Crochet JY *et al*. A revision of *Aceratherium blanfordi* Lydekker, 1884 (Mammalia: Rhinocerotidae) from the Early Miocene of Pakistan: postcranials as a key: Miocene rhinocerotids from Pakistan. *Zoological Journal of the Linnean Society* 2010;**160**:139–94. https://doi.org/10.1111/j.1096-3642.2009.00597.x

Antoine PO, Métais G, Orliac MJ *et al*. Mammalian neogene biostratigraphy of the sulaiman province, Pakistan. In: Fortelius M, Wang X, Flynn L (eds), *Fossil Mammals of Asia*. New York: Columbia University Press, 2013;400–422.

Cerdeño E. Cladistic analysis of the Family Rhinocerotidae (Perissodactyla). *American Museum Novitates* 1995;**3143**:1–25.

Cerdeño E. *Prosantorhinus*, the small teleoceratine rhinocerotid from the Miocene of Western Europe. *Geobios* 1996;**29**:111–24. https://doi.org/10.1016/s0016-6995(96)80077-5

Cerdeño E, Sanchez B. Intraspecific variation and evolutionary trends of *Alicornops simorrense* (Rhinocerotidae) in Spain. *Zoologica Scripta* 2000;**29**:275–305. https://doi.org/10.1046/j.1463-6409.2000.00047.x

Deng T. New material of *Hispanotherium matritense* (Rhinocerotidae, Perissodactyla) from Laogou of Hezheng County (Gansu, China), with special reference to the Chinese Middle Miocene elasmotheres. *Geobios* 2003;**36**:141–50. https://doi.org/10.1016/s0016-6995(03)00003-2

Deng T. A new species of the rhinoceros *Alicornops* from the Middle Miocene of the Linxia Basin, Gansu, China. *Palaeontology* 2004;**47**:1427–39. https://doi.org/10.1111/j.0031-0239.2004.00420.x

Deng T. New cranial material of *Shansirhinus* (Rhinocerotidae, Perissodactyla) from the Lower Pliocene of the Linxia Basin in Gansu, China. *Geobios* 2005;**38**:301–13. https://doi.org/10.1016/j.geobios.2003.12.003

Fortelius M, Solounias N. Functional characterization of ungulate molars using the abrasion-attrition wear gradient: a new method for reconstructing paleodiets. *American Museum Novitates* 2000;**3301**:1–36. https://doi.org/10.1206/0003-0082(2000)301<0001:fcoumu>2.0.co;2

Geraads D, Miller E. *Brachypotherium minor* n sp, and other Rhinocerotidae from the Early Miocene of Buluk, Northern Kenya. *Geodiversitas* 2013;**35**:359–75. https://doi.org/10.5252/g2013n2a5

Guérin C. Les rhinocéros (Mammalia, Perissodactyla) du Miocène terminal au Pléistocène supérieur en Europe occidentale Comparaison avec les espèces actuelles (fascicule 1). *Travaux et Documents des Laboratoires de Géologie de Lyon* 1980;**79**:1–1184.

Harrison T, Delson E, Jian G. A new species of *Pliopithecus* from the middle Miocene of China and its implications for early catarrhine zoogeography. *Journal of Human Evolution* 1991;**21**:329–61. https://doi.org/10.1016/0047-2484(91)90112-9

Heissig K. Die obermiozäne Fossil-Lagerstätte Sandelzhausen. 5. Rhinocerotidae (Mammalia), Systematik und Ökologie. *Mitteilungen der Bayerischen Staatssammlung für Paläontologie und historische Geologie,* 1972;**12**:57–81.

Heissig K. *Prosantorhinus* pro *Brachypodella* HEISSIG 1972 (Rhinocerotidae, Mammalia) (non *Brachypodella* BECK 1837 [Gastropoda]). *Mitteilungen der Bayerischen Staatssammlung für Paläontologie und historische Geologie* 1974;**14**:37.

Heissig K. Family Rhinocerotidae. In: Rössner GE., Heissig K. (eds), *The Miocene Land Mammals of Europe*. Munich: Verlag Dr. F. Pfeil, 1999, 175–188.

Heissig K. Revision of the European species of *Prosantorhinus* HEISSIG, 1974 (Mammalia, Perissodactyla, Rhinocerotidae). *Fossil Imprint* 2017;**73**:236–74. https://doi.org/10.2478/if-2017-0014

Heissig K, Fejfar O. Die Säugetiere aus dem Untermiozän von Tuchořice in Nordwestböhmen.—I. Die fossilen Nashörner (Mammalia, Rhinocerotidae). *Acta Musei Nationalis Pragae. Hist. Nat* 2007;**63**:19–64.

Hullot M, Laurent Y, Merceron G, *et al.* Paleoecology of the Rhinocerotidae (Mammalia, Perissodactyla) from Béon 1, Montréal-du-Gers (late early Miocene, SW France): Insights from dental microwear texture analysis, mesowear, and enamel hypoplasia[J]. *Palaeontologia Electronica*, 2021;**24**(2):a27.

Jame C, Tissier J, Maridet O *et al.* Early Agenian rhinocerotids from Wischberg (Canton Bern, Switzerland) and clarification of the systematics of the genus *Diaceratherium*. *PeerJ* 2019;**7**:e7517. https://doi.org/10.7717/peerj.7517

Lu XK, Deng T, Pandolfi L. Reconstructing the phylogeny of the hornless rhinoceros Aceratheriinae. *Frontiers in Ecology and Evolution* 2023;**11**:1005126.

Osborn HF. Phylogeny of the rhinoceroses of Europe. *Bulletin of the American Museum of Natural History* 1900;**13**:229–67.

Prothero DR. *The Evolution of North American Rhinoceroses*. Cambridge: Cambridge University Press, 2005; 1–218.

Prothero DR, Manning E, Hanson CB. The phylogeny of the Rhinocerotoidea (Mammalia, Perissodactyla). *Zoological Journal of the Linnean Society* 1986;**87**:341–66. https://doi.org/10.1111/j.1096-3642.1986.tb01340.x

Qiu ZX, Wang BY, Deng T. Mammal fossils from Yagou, Linxia Basin, Gansu, and related stratigraphic problems. *Vertebrata PalAsiatica* 2004;**42**:276–96.

Schellhorn R. A potential link between lateral semicircular canal orientation, head posture, and dietary habits in extant rhinos (Perissodactyla, Rhinocerotidae). *Journal of Morphology* 2018;**279**:50–61. https://doi.org/10.1002/jmor.20753

Schellhorn R. Stiffening in the carpus of *Prosantorhinus germanicus* (Perissodactyla, Rhinocerotidae) from Sandelzhausen (Germany). *Paläontologische Zeitschrift* 2021;**95**:531–6. https://doi.org/10.1007/s12542-021-00574-7

Schellhorn R, Schlösser M. *A partial distal forelimb of a woolly rhino (Coelodonta antiquitatis) from Wadersloh (Westphalia, Germany) and insights from bone compactness*, 2021;**94**:15–35.

Sizov A, Klementiev A, Antoine PO. An Early Miocene skeleton of *Brachydiceratherium* Lavocat, 1951 (Mammalia, Perissodactyla) from the Baikal area, Russia, and a revised phylogeny of Eurasian teleoceratines. *bioRxiv* 2022. https://doi.org/10.1101/2022.07.06.498987

Sun D, Deng T, Lu X *et al.* A new elasmothere genus and species from the middle Miocene of Tongxin, Ningxia, China, and its phylogenetic relationship. *Journal of Systematic Palaeontology* 2023;**21**:2236619.

Swofford DL. 2002. *PAUP*. Phylogenetic Analysis Using Parsimony (*and Other Methods) Version 4*. Sunderland, Massachusetts: Sinauer Associates.

Tütken T, Vennemann T. Stable isotope ecology of Miocene large mammals from Sandelzhausen, southern Germany. *Paläontologische Zeitschrift* 2009;**83**:207–26. https://doi.org/10.1007/s12542-009-0011-y

Wang J. 2021. *Vegetation History in Northern China and its Response to Critical Geological and Environmental Events since the Neogene*. Beijing: Institute of Vertebrate Paleontology and Paleoanthropology, University of Chinese Academy of Sciences.

Wang S, Zong L, Yang Q *et al.* Biostratigraphic subdividing of the Neogene Dingjia'ergou mammalian fauna, Tongxin County, Ningxia Province, and its background for the uplift of the Tibetan Plateau. *Quaternary Sciences* 2016;**36**:789–809.

You Y, Huber M, Müller RD *et al.* Simulation of the middle miocene climate optimum. *Geophysical Research Letters* 2009;**36**:L04702.

Zachos J, Pagani M, Sloan L *et al.* Trends, rhythms, and aberrations in global climate 65 Ma to present. *Science* 2001;**292**:686–93. https://doi.org/10.1126/science.1059412

Zachos JC, Dickens GR, Zeebe RE. An early Cenozoic perspective on greenhouse warming and carbon-cycle dynamics. *Nature* 2008;**451**:279–83. https://doi.org/10.1038/nature06588